International Journal of Minerals, Metallurgy and Materials
Volume 22, Number 8, August 2015, Page 884
DOI: 10.1007/s12613-015-1146-3

Molten salt synthesis of mullite nanowhiskers using different silica sources

Tao Yang[1,2)], *Peng-long Qiu*[1)], *Mei Zhang*[1)], *Kuo-Chih Chou*[1,2)], *Xin-mei Hou*[1,2)], *and Bai-jun Yan*[1)]

1) Department of Metallurgical Physical Chemistry, School of Metallurgical and Ecological Engineering, University of Science and Technology Beijing, Beijing 100083, China

2) State Key Laboratory of Advanced Metallurgy, University of Science and Technology Beijing, Beijing 100083, China

(Received: 8 June 2014; revised: 23 October 2014; accepted: 27 October 2014)

Abstract: Mullite nanowhiskers with Al-rich structure were prepared by molten salt synthesis at 1000°C for 3 h in air using silica, amorphous silica, and ultrafine silica as the silica sources. The phase and morphology of the synthesized products were investigated by X-ray diffraction, scanning electron microscopy, energy dispersive spectroscopy, and transmission electron microscopy. A thermogravimetric and differential thermal analysis was carried out to determine the reaction mechanism. The results reveal that the silica sources play an important role in determining the morphology of the obtained mullite nanowhiskers. Clusters and disordered arrangements are obtained using common silica and amorphous silica, respectively, whereas the use of ultrafine silica leads to highly ordered mullite nanowhiskers that are 80–120 nm in diameter and 20–30 μm in length. Considering the growth mechanisms, mullite nanowhiskers in the forms of clusters and highly ordered arrangements can be attributed to heterogeneous nucleation, whereas disordered mullite nanowhiskers are obtained by homogenous nucleation.

Keywords: mullite; nanowhiskers; morphology; silica; molten salt synthesis; reaction mechanisms

1. Introduction

Mullite is widely used as refractory lining and structural ceramic because of its attractive properties, such as high-temperature strength, creep resistance, and low thermal expansion coefficient. A study published recently [1] indicates that a synthetic analogue of mullite is an efficient substitute for commercial Pt-based catalysts used to reduce the amount of pollution generated by diesel engines. This finding will undoubtedly accelerate the development of the market for mullite compounds. Mullite whiskers have attracted attention as a reinforcement for high-temperature structure materials. At present, surface-enhanced Raman scattering (SERS) is one of the most powerful analytical tools for chemical and biological detection because of its high sensitivity and specificity [2–5]. Usually, Au and Ag are conventional SERS substrates for ultra-sensitive detection [6–8]. It is well known that mullite is chemically stable under corrosion conditions, and therefore, highly ordered mullite nanowhiskers decorated with Au and Ag nanoparticles can be used as a possible SERS substrate under corrosion conditions.

Various methods have been applied to prepare mullite whiskers including the sol–gel method [9–10], high-energy ball milling [11–13], and the thermal decomposition of minerals [14]. Among these methods, molten salt synthesis (MSS) is widely employed to synthesize functional and structural ceramics because it requires low reaction temperatures and leads to products with a homogeneous morphology [15–16]. Mullite nanowires have been synthesized by MSS before [17–21]. However, the previous studies mainly focused on the preparation of mullite using different molten salt systems. It was pointed out that silica with different crystal structures plays an important role in determining the morphology of mullite whiskers [21], but no further study has been reported.

In this paper, mullite nanowhiskers were prepared in a Na_2SO_4 molten salt system with B_2O_3 addition using different silica sources, namely, common silica, amorphous silica,

Corresponding author: Bai-jun Yan E-mail: baijunyan@ustb.edu.cn

and ultrafine silica. A reaction mechanism was proposed based on the experimental results. Especially, the influence of the silica sources on the formation of highly ordered mullite naowhiskers was discussed for the first time. This research will promote a new and comprehensive understanding of the synthesis of highly ordered mullite whiskers by MSS. In addition, it will pave a way for the practical application of mullite whiskers as substrates for SERS under corrosion conditions.

2. Experimental

2.1. Materials and methods

Various silica sources, including common silica (SiO_2, purity > 99%) with an average particle size of 150 μm, amorphous silica (SiO_2, purity > 99%), and an ultrafine silica powder (SiO_2, purity > 99%) with an average particle size of 10 μm, were employed in the experiments. Aluminum sulfate hydrate [$Al_2(SO_4)_3{\cdot}18H_2O$, purity > 99%] was used as the alumina precursor. Sodium sulfate (Na_2SO_4, purity > 99%) with boric oxide (B_2O_3, purity > 99%) as additive was selected as the molten salt system.

Firstly, $Al_2(SO_4)_3{\cdot}18H_2O$ (200 g) was calcined at 300°C for 3 h to remove the crystal water. $Al_2(SO_4)_3$ and Na_2SO_4 (with a mass ratio of 34:66) were mixed according to the $Al_2(SO_4)_3$–Na_2SO_4 phase diagram. The mixture of silica source, $Al_2(SO_4)_3$, and B_2O_3 (with a molar ratio of 6:6:1) was mixed with Na_2SO_4 by ball milling. Then, the mixture was put in a high-purity magnesium oxide crucible and heated in an electric furnace to 1000°C for 3 h under air atmosphere. After cooling to room temperature, the obtained product was washed with 90°C water to remove the sulfate and then etched using 20wt% hydrofluoric acid (HF) for 1 h to remove the residual silica. Finally, a white powder was obtained.

2.2. Phase and microstructure characterization

The crystal structure of the samples was examined by X-ray diffraction (XRD) on a TTRⅢ diffractometer using Cu K_α radiation over a 2θ range from 10° to 90° (M21XVHF22, Japan). The morphology of the samples was examined by scanning electron microscopy, SEM (ZEISS SUPRATM 55, Germany), and transmission electron microscopy, TEM (HITACHI H8100, Japan). Further structural characterization was performed by HRTEM (JEM 2010, Japan) and selected area electron diffraction (SAED). A thermogravimetric and differential thermal analysis, TG-DTA (NETZSCH STA 449 C, Germany), was carried out to investigate the reaction mechanism.

3. Results and discussion

3.1. Phase and microstructure

Fig. 1 shows the microstructures of the synthesized samples using various silica sources. As shown in Figs. 1(a) and 1(b), for the samples obtained using common silica as the silica source, clusters of needlelike whiskers are formed with some bulk substrate enwrapped in the center. The length of the nanowhiskers is below 10 μm. Energy dispersive spectroscopy (EDS) results (inset in Fig. 1(a)) reveal that the whiskers are composed of Al, Si, and O. Further quantitative analysis shows that the atomic ratio of Al:Si is close to 4:1, which is very similar to the ratio in $Al_2(Al_{2.8}Si_{1.2})O_{9.6}$. Regarding the composition of the core of the whiskers, the EDS (inset in Fig. 1(b)) reveals that it is composed of Si and O with an atomic ratio of O:Si of 2:1. Therefore, mullite clusters with undissolved silica enwrapped in the center are formed using common silica as the silica source, which is consistent with a previous study [21].

Figs. 1(c) and 1(d) display SEM micrographs and EDS results for the product synthesized using amorphous silica as the silica source. The EDS result (inset in Fig. 1 (d)) demonstrates that the whiskers are mullite with an atomic ratio of Al:Si of about 4:1. The mullite whiskers appear to have a uniform microstructure morphology and their length goes up to more than 20 μm. However, the overall arrangement of the nanowhiskers is disordered.

Figs. 1(e) and 1(f) show SEM micrographs and EDS results of samples obtained using ultrafine silica powder as the silica source. It can be seen that mullite whiskers with a preferred orientation are synthesized on a large scale. In addition, the whiskers appear to have a uniform morphology (inset in Fig. 1(e)). From the side view (Fig. 1(f)), it can be seen that the length of the nanowhiskers is 20–30 μm, with a highly ordered growth orientation. The EDS result (inset in Fig. 1 (f)) reveals that the whiskers are mullite with an atomic ratio of Al:Si of about 4:1. Therefore, the formula of the obtained product is $Al_2(Al_{2.8}Si_{1.2})O_{9.6}$. Boron is not detected in the nanowhiskers.

XRD patterns of the as-synthesized nanowhiskers are shown in Fig. 2. It can be seen that mullite and quartz phases exist in the product when using common silica as the silica source (Fig. 2(a)). By contrast, only mullite is detected if amorphous silica or ultrafine silica are used as shown in Figs. 2(b) and 2(c). The characteristic peaks of mullite are indexed to the orthorhombic structure of $Al_2(Al_{2.8}Si_{1.2})O_{9.6}$, a kind of Al-rich mullite with the cell parameters: a = 0.7588, b = 0.7688, and c = 0.28895 nm (PDF#79-1275).

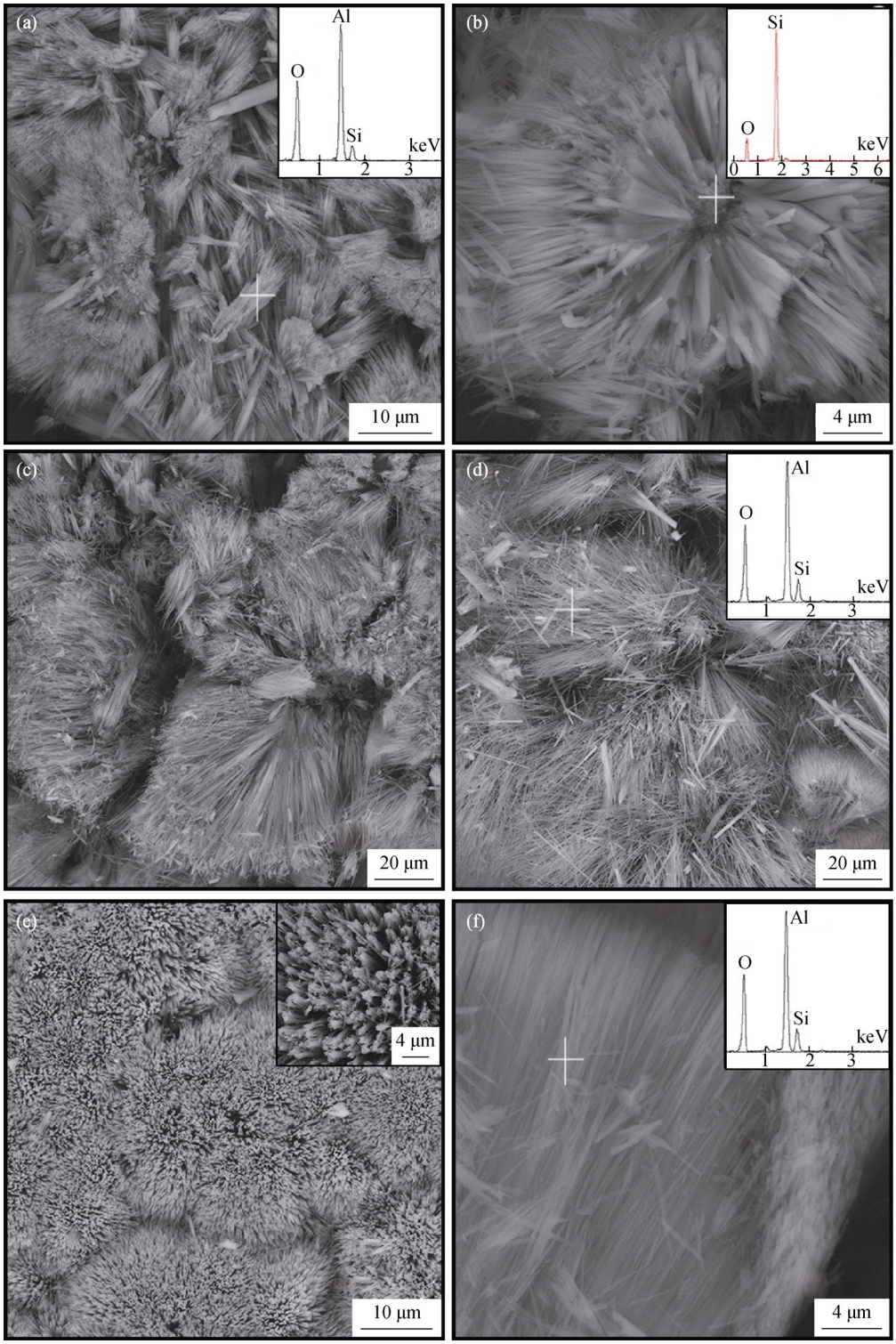

Fig. 1. SEM images and EDS results of mullite whiskers synthesized using different silica sources: (a,b) SEM images of mullite nanowhiskers obtained using common silica as the silica source (the insets are the EDS results of the nanowhiskers); (c,d) SEM images of mullite nanowhiskers obtained using amorphous silica as the silica source (the inset is the EDS of the nanowhiskers); (e,f) SEM images of mullite nanowhiskers obtained using ultrafine silica powder as the silica source (the inset in (e) is the SEM image of the nanowhiskers at high magnification; the inset in (f) is the EDS of the nanowhiskers).

Fig. 3 shows TEM images of samples synthesized using various silica sources. Figs. 3(a) and 3(b) show that the microstructure of mullite whiskers obtained using common silica as the silica source is single crystalline while their

morphology is non-uniform. The microstructure of the product synthesized using amorphous silica as the silica source is shown in Figs. 3(c) and 3(d). As shown in Fig. 3(c), the diameter of the whiskers is in the range of 80–120 nm. HRTEM images combined with SAED results (Fig. 3(d)) indicate that the whiskers are also single crystalline. In addition, the interplanar spacings detected from the legible lattice fringes along the axis of the whisker are 0.540 nm, which are quite similar to that of the (110) planes of $Al_2(Al_{2.8}Si_{1.2})O_{9.6}$. This indicates that the preferential growth direction of the nanowhiskers is parallel to the (110) planes. Figs. 3(e) and 3(f) show TEM images of mullite whiskers obtained using ultrafine silica powder as the silica source. It can be seen that the whiskers do not only possess a uniform morphology, with a diameter in the range of 80–120 nm, but also are single crystalline. All the SAED patterns of mullite nanowhiskers obtained using different silica sources can be indexed to the (110) and (001) planes (inset in Figs. 3(b), 3(d), and 3(f)), verifying that the preferential growth direction of the nanowhiskers is parallel to the (110) planes.

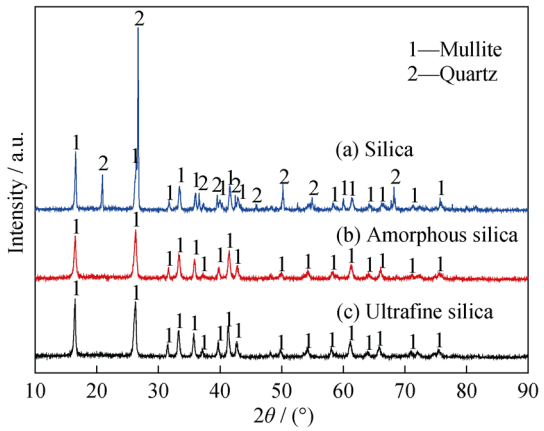

Fig. 2. XRD patterns of products synthesized using various silica sources.

3.2. TG-DTA curves

Fig. 4 shows the TG-DTA curves of samples prepared using ultrafine silica at temperatures from room temperature to 1300°C in air. The TG curve indicates that the sample loses weight slightly from 100 to 400°C. The corresponding DTA curve exhibits a small endothermic peak at 250°C, which is possibly caused by the dehydration reaction. There are two possible reasons to explain this phenomenon. The first one is that $Al_2(SO_4)_3$ tends to absorb moisture from the atmosphere, and the second one is that the dehydration of $Al_2(SO_4)_3{\cdot}18H_2O$ does not occur completely during the calcination process. Upon increasing the temperature, an endothermic peak appears at approximately 650°C due to the melting of Na_2SO_4 and $Al_2(SO_4)_3$ [22]. The TG curve shows that the material apparently begins to lose weight at about 800°C, which is attributed to the partial decomposition of $Al_2(SO_4)_3$ according to the following equation:

$$Al_2(SO_4)_3 \rightarrow Al_2O_3 + 3SO_3\uparrow \quad (1)$$

Since the decomposition of $Al_2(SO_4)_3$ (Eq. (1)) is an endothermic process, the endothermic peak appears at 800°C in the corresponding DTA curve. If the temperature is increased further, mullite is formed according to the following equation:

$$6SiO_2(l) + 12Al_2(SO_4)_3(l) \rightarrow 5Al_2(Al_{2.8}Si_{1.2})O_{9.6}(s) + 36SO_3\uparrow \quad (2)$$

Since mullite formation is an endothermic process [23] with a slow reaction rate, some endothermic peaks appear at 950–1100°C. At the same time, the sample obviously loses weight within this temperature range because of the formation of the gas product according to Eq. (2). At temperatures above 1100°C, mullite tends to decompose according to the following equation [23]:

$$3Al_2O_3{\cdot}2SiO_2(s) + 3Na_2SO_4(l) + 4SiO_2(l) \rightarrow 6NaAlSiO_4(s) + 3SO_3\uparrow \quad (3)$$

Therefore, mullite can be synthesized at 950–1100°C in Na_2SO_4 flux.

3.3. Formation mechanism of mullite nanowhiskers using different silica sources

From the above experiment, it can be seen that silica plays an important role in determining the morphology of mullite whiskers. A similar phenomenon has been reported in the literature for mullite synthesis through a solid-state reaction [21]. However, the formation mechanism for the MSS method has not been reported up to now. In the following section, we will discuss the formation mechanism and the effect of the silica sources on the morphology of mullite whiskers in Na_2SO_4 flux.

It is well known that dissolved chemical reagents present in the molten salt system can easily react with each other and transform via precipitation [18]. According to the $Al_2(SO_4)_3$–Na_2SO_4 phase diagram, the eutectic point of this system is 650°C. Therefore, $Al_2(SO_4)_3$ can be dissolved at low temperatures. Upon increasing the temperature, the material tends to decompose at about 800°C to form Al_2O_3 (Eq. (1)) [23]. Considering that the melting point of Al_2O_3 is higher than that of silica, the former material may crystallize from the molten system. However, the Al_2O_3 molecules are wrapped by dissolved silica, which prevents them from contacting each other and nucleating. Therefore, there are no characteristic peaks for Al_2O_3 in the XRD pattern (Fig. 3). From the above analysis, it can be concluded that Al_2O_3

molecules with high reactivity are not the limiting factor for mullite formation. Instead, the process is controlled by the dissolution rate of silica and silica further affects the morphology of the mullite whiskers.

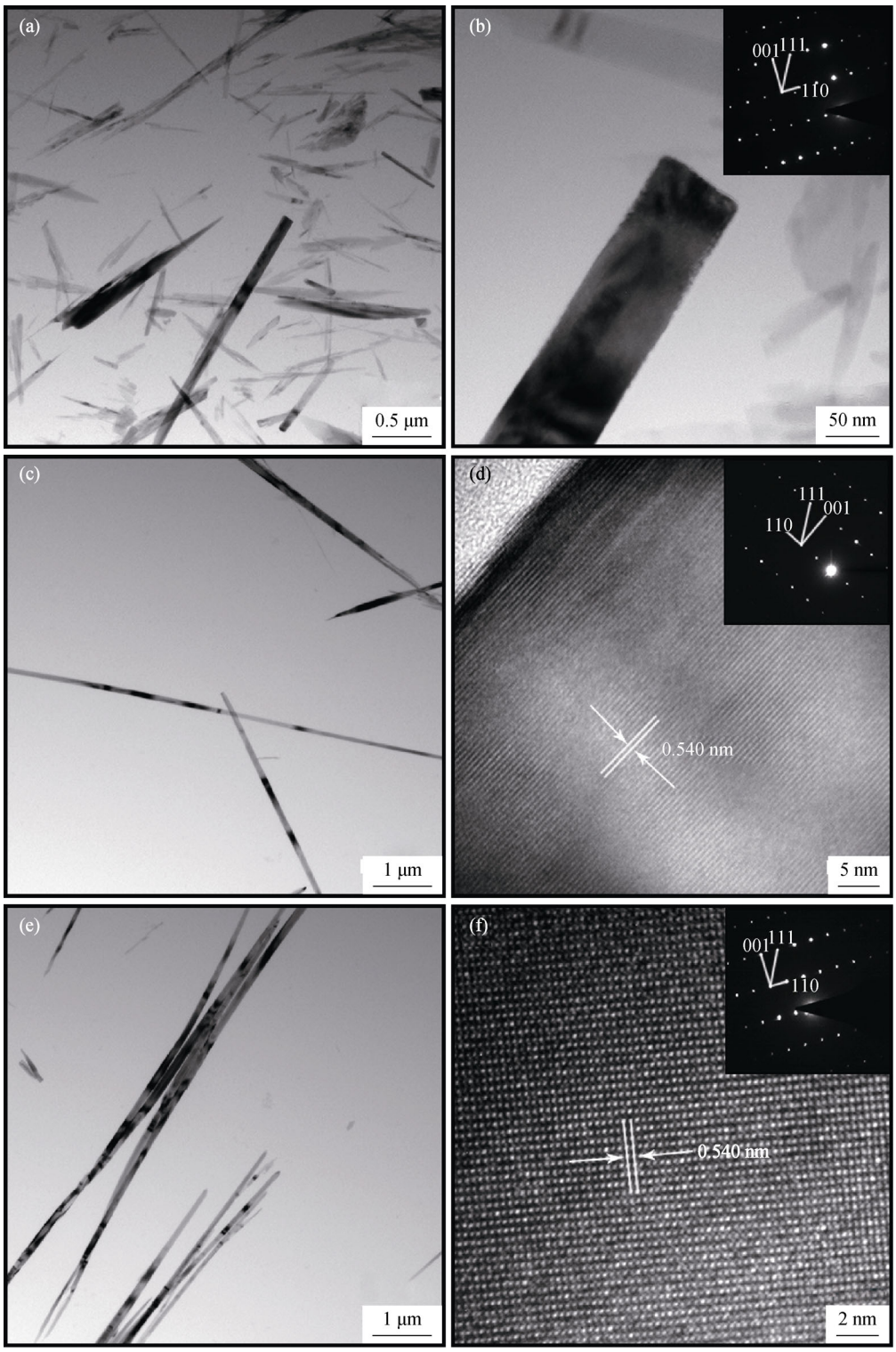

Fig. 3. TEM and HRTEM images of mullite whiskers obtained using different silica sources: (a,b) TEM images of mullite nanowhiskers obtained using common silica as the silica source (the inset in (b) is the SAED pattern of the nanowhiskers); (c,d) TEM images of mullite nanowhiskers obtained using amorphous silica as the silica source (the inset in (d) is the SAED pattern of the nanowhiskers); (e,f) TEM images of mullite nanowhiskers obtained using ultrafine silica powder as the silica source (the inset in (f) is the SAED pattern of the nanowhiskers).

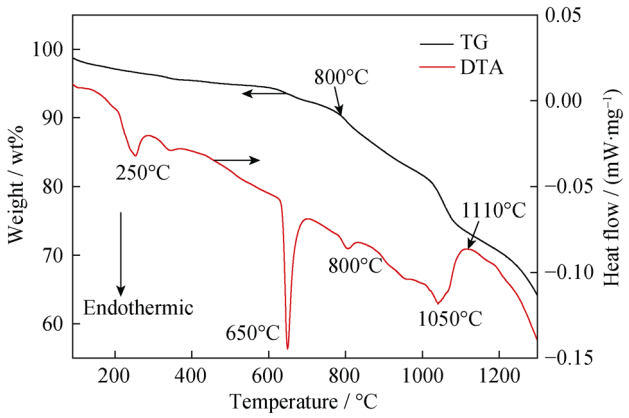

Fig. 4. TG-DTA curves of the powder from room temperature to 1300°C in air.

A schematic diagram of the formation mechanism of mullite whiskers using common silica as the silica source is presented in Fig. 5. Only the outer layer of common silica is dissolved because of its relatively low reactivity. Owing to the lower nucleation barrier at the interface, mullite tends to nucleate at the outer layer of common silicon and grows along the {110} direction because it is the close-packed plane. After a certain time, the mullite whiskers are formed. Since the formation rate of the mullite whiskers is faster than the dissolution rate of common silica, the remaining silica is wrapped by mullite whiskers so that clusters of mullite whiskers with undissolved silica as the core are formed, as shown in Figs. 2(a) and 2(b). This process can be described as a heterogeneous nucleation.

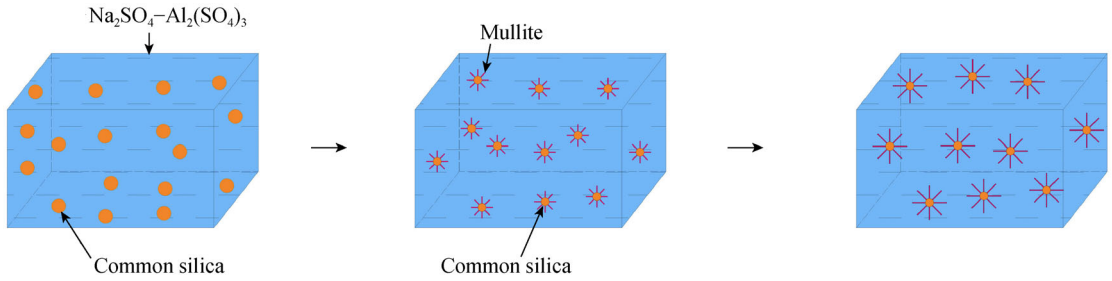

Fig. 5. Schematic diagram of the mullite whisker formation mechanism using common silica as the silica source.

Fig. 6 is a schematic diagram describing the formation mechanism of mullite whiskers using amorphous silica as the silica source. It is a homogeneous nucleation process because amorphous silica is completely dissolved in the Na_2SO_4 flux as a result of its strong dissolution capability [23]. At a longer time, the nucleation of mullite whiskers is promoted and isolated mullite whiskers form.

A schematic diagram of the mullite whisker formation mechanism using ultrafine silica as the silica source is shown in Fig. 7. Since the dissolution rate of ultrafine silica is between the rates of common silica and amorphous silica, ultrafine silica cannot be dissolved completely at the initial stage. At the same time, the density of silica (2.2 g/mL) is greater than that of the $Al_2(SO_4)_3$–Na_2SO_4 flux (1.68 g/mL),

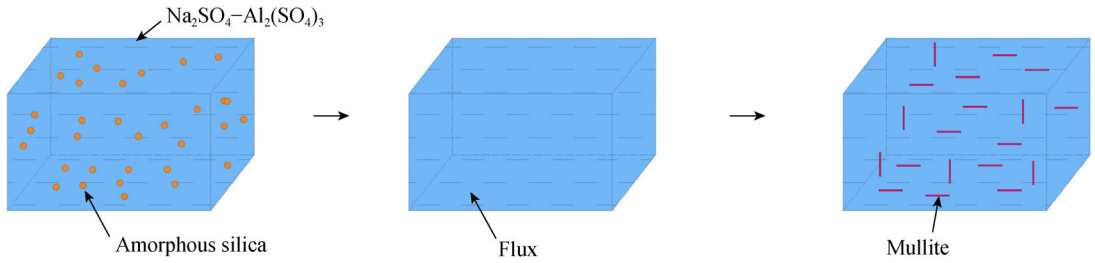

Fig. 6. Schematic diagram of the mullite whisker fomation mechanism using amorphous silica as the silica source.

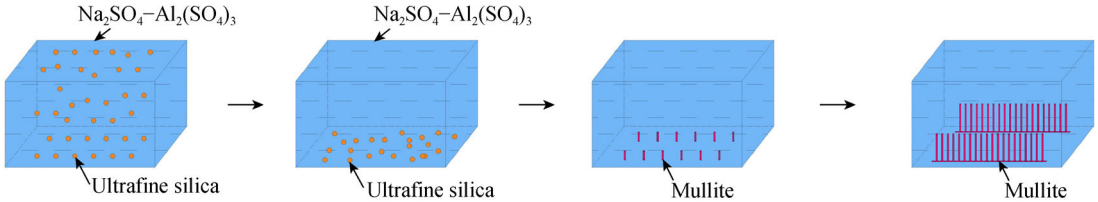

Fig. 7. Schematic diagram of the mullite whisker formation mechanism using ultrafine silica as the silica source.

and the addition of B_2O_3 further decreases the viscosity of the flux by several orders of magnitude [24]. Therefore, a part of the ultrafine silica particles sinks to the bottom of the crucible. Due to the lower barrier for nucleation at the interface with silica, the mullite nuclei are likely to be initially formed at that interface and then grow along the {110} direction. With the extension of time, silica is continuously dissolved in the molten salt and the concentration increases. This promotes the growth of mullite whiskers so that finally a large amount of highly ordered whiskers are synthesized.

4. Conclusions

Mullite nanowhiskers with Al-rich and single-crystalline structure are prepared by MSS at 1000°C for 3 h in air. The effect of various silica sources on the morphology of mullite is especially discussed. The results show that disordered mullite nanowhiskers are obtained in the samples prepared using amorphous silica as the silica source, whereas clusters of mullite nanowhiskers are obtained in the samples synthesized using common silica. Many highly ordered mullite nanowhiskers are synthesized using ultrafine silica as the silica source. The formation mechanism of the disordered mullite nanowhiskers obtained from amorphous silica is based on homogeneous nucleation, whereas mullite nanowhiskers in the form of clusters and highly ordered arrangements are obtained by heterogeneous nucleation.

Acknowledgements

The authors express their appreciation to the New Century Excellent Talents in Universities (No. NECT−12−0779), the Fundamental Research Funds for the Central Universities (No. FRF-SD-13-006A), and the Program for Changjiang Scholars and Innovative Research Team in Universities (No. IRT1207) for financial support.

References

[1] W. Wang, G. McCool, N. Kapur, G. Yuan, B. Shan, M. Nguyen, U.M. Graham, B.H. Davis, G. Jacobs, K. Cho, and X.K. Hao, Mixed-phase oxide catalyst based on Mn-Mullite (Sm, GD) Mn_2O_5 for NO oxidation in diesel exhaust, *Science*, 337(2012), No. 6096, p. 832.

[2] S. Tian, Q. Zhou, C.H. Li, Z.M. Gu, J.R. Lombardi, and J.W. Zheng, Exploring the chemical enhancement of surface-enhanced raman scattering with a designed silver/Silica cavity substrate. *J. Phys. Chem. C*, 117(2012), No. 1, p. 556.

[3] X.M. Qian, X.H. Peng, D.O. Ansari, Q. Yin-Goen, G.Z. Chen, D.M. Shin, L. Yang, A.N. Young, M.D. Wang, and S.M. Nie, *In vivo* tumor targeting and spectroscopic detection with surface-enhanced Raman nanoparticle tags, *Nat. Biotechnol.*, 26(2008), No. 1, p. 83.

[4] F. Casadio, M. Leona, J.R. Lombardi, and R. Van Duyne. Identification of organic colorants in fibers, paints, and glazes by surface enhanced Raman spectroscopy, *Acc. Chem. Res.*, 43(2010), No. 6, p. 782.

[5] J.F. Li, Y.F. Huang, Y. Ding, Z.L. Yang, S.B. Li, X.S. Zhou, F.R. Fan, W. Zhang, Z.Y. Zhou, D.Y. Wu, B. Ren, Z.L. Wang, and Z.Q. Tian, Shell-isolated nanoparticle-enhanced Raman spectroscopy, *Nature*, 464(2010), No. 7284, p. 392.

[6] A.M. Schwartzberg, C.D. Grant, A. Wolcott, C.E. Talley, T.R. Huser, R. Bogomolni, and J.Z. Zhang, Unique gold nanoparticle aggregates as a highly active surface-enhanced Raman scattering substrate, *J. Phys. Chem. B*, 108(2004), No. 50, p. 19191.

[7] S. Sasic, T. Itoh, and Y. Ozaki, Detailed analysis of single-molecule surface-enhanced resonance Raman scattering spectra of Rhodamine 6G obtained from isolated nano-aggregates of colloidal silver, *J. Raman Spectrosc.*, 36(2005), No. 6-7, p. 593.

[8] I. Yoon, T. Kang, W. Choi, J. Kim, Y. Yoo, S.W. Joo, Q.H. Park, H. Ihee, and B. Kim, Single nanowire on a film as an efficient SERS-active platform, *J. Am. Ceram. Soc.*, 131(2008), No. 2, p. 758.

[9] Y.B. Zhang, Y.P. Ding, J.Q. Gao, and J.F. Yang. Mullite fibres prepared by sol-gel method using polyvinyl butyral, *J. Eur. Ceram. Soc.*, 29(2009), No. 6, p. 1101.

[10] B. Bagchi, S. Das, A. Bhattacharya, R. Basu, and P. Nandy, Nanocrystalline mullite synthesis at a low temperature: effect of copper ions, *J. Am. Ceram. Soc.*, 92(2009), No. 3, p. 748.

[11] L.B. Kong, T.S. Zhang, J. Ma, and F.Y.C. Boey, Mullitization behavior and microstructural development of B_2O_3–Al_2O_3–SiO_2 mixtures activated by high-energy ball milling, *Solid State Sci.*, 11(2009), No. 8, p. 1333.

[12] T.S. Zhang, L.B. Kong, Z.H. Du, J. Ma, and S. Li, *In situ* interlocking structure in gel-derived mullite matrix induced by mechanoactivated commercial mullite powders, *Scripta Mater.*, 63(2010), No. 11, p. 1132.

[13] T.S. Zhang, L.B. Kong, Z.H. Du, J. Ma, and S. Li, Tailoring the microstructure of mechanoactivated Al_2O_3 and SiO_2 mixtures with TiO_2 addition, *J. Alloys Compd.*, 506(2010), No. 2, p. 777.

[14] J.F. Li, H. Lin, J.B. Li, and J. Wu. Effects of different potassium salts on the formation of mullite as the only crystal phase in kaolinite, *J. Eur. Ceram. Soc.*, 29(2009), No. 14, p. 2929.

[15] S. Okada, T. Shishido, T. Mori, K. Iizumi, K Kudou, and K. Nakajima, Crystal growth of $MgAlB_{14}$-type compounds using metal salts and some properties, *J. Alloys Compd.*, 458(2008), No. 1, p. 297.

[16] Y.M. Park, T.Y. Yang, S.Y. Yoon, R. Stevens, and H.C. Park, Mullite whiskers derived from coal fly ash, *Mater. Sci. Eng. A*, 454(2007), p. 518.

[17] P.Y. Zhang, J.C. Liu, H.Y. Du, Z.Q. Li, S. Li, S. Li, and R. Xu, Molten salt synthesis of mullite whiskers from various alumina precursors, *J. Alloys Compd.*, 491(2010), No. 1, p. 447.

[18] R. El Ouatib, S. Guillemet, B. Durand, A. Samdi, L. Er Rakho, and R. Moussa, Reactivity of aluminum sulfate and silica in molten alkali-metal sulfates in order to prepare mullite, *J. Eur. Ceram. Soc.*, 25(2005), No. 1, p. 73.

[19] L.B. Kong, Y.B. Gan, J. Ma, T.S. Zhang, F. Boey, and R.F. Zhang, Mullite phase formation and reaction sequences with the presence of pentoxides, *J. Alloys Compd.*, 351(2003), No. 1, p. 264.

[20] B.M. Kim, Y.K. Cho, S.Y. Yoon, R. Stevens, and H.C. Park, Mullite whiskers derived from kaolin, *Ceram. Int.*, 35(2009), No. 2, p. 579.

[21] P.Y. Zhang, J.C. Liu, H.Y. Du, Z.Q. Li, S. Li, and C. Chen. Influence of silica sources on morphology of mullite whiskers in Na_2SO_4 flux, *J. Alloys Compd.*, 484(2009), No. 1, p. 580.

[22] E.M. Levin and H.F. McMurdie, *Phase Diagrams for Ceramists* 1975 *Supplement*, American Ceramic Society, Inc., Columbus, OH, 1975, p. 318.

[23] B. Zhu, X. Li, R. Hao, and H. Wang, Thermodynamics study on mullite preparation in molten sodium sulfate. *J. Chin. Ceram. Soc.*, 34(2006), No. 1, p. 76.

[24] X.H. Huang, J.L. Liao, K. Zheng, H.H. Hu, F.M. Wang, Z.T. Zhang, Effect of B_2O_3 addition on viscosity of mould slag containing low silica content, *Ironmaking Steekmaking*, 41(2014), No. 1, p. 67.